Transformation of Satellite Data into Air Temperature: A Study in La Rioja, Argentina.

RODOLFO DEMATTE[1,2], JOSEFINA HUESPE[2]

[1]Instituto de Energías Naturales Renovables Centro de Investigación e Innovación Tecnológica – CENIIT
Universidad Nacional de La Rioja
Av. Luis Vernet 1000, La Rioja -Capital
(5300) La Rioja
ARGENTINA

[2]Unidad Investigadora: Epistemología, Lógica y Ciencias Básicas. Grupo IEMI.
Universidad Tecnológica Nacional
Facultad Regional Mendoza
Coronel Rodríguez 273, Ciudad – Capital
(M5500) Mendoza
ARGENTINA

Abstract: - This study examines the differences between air temperature (Ta) and land surface temperature (LST), focusing on urban (UA) and non-urban area (NUA) characteristics in La Rioja, Argentina. Urban air temperature (Ta_{UA}) data were collected from the National Meteorological Service station at the La Rioja airport (-29.38 S, -66.79 W). In comparison, rural data (Ta_{NUA}) were obtained from a meteorological station 10 km away in a non-urban area (-29.47 S, -66.78 W). LST data were sourced from NASA's MERRA-2 database. Correction methods were developed to transform LST measurements into values comparable to Ta_{UA} and Ta_{NUA}, enhancing accuracy when analyzing urban heat island effects. The study yielded equations with high correlations (R^2 = 0.87–0.91), which enabled improved characterization of temperature differences across UA and NUA. These methods contribute to better understanding and quantifying the urban heat island phenomenon by addressing discrepancies between surface and atmospheric temperatures. This study not only improves the characterization of temperature differences between UA and NUA in La Rioja, Argentina, but also provides a valuable tool for agriculture, public health, and urban planning by enabling more accurate air temperature (Ta_{UA} and Ta_{NUA}) estimations from satellite data, particularly in regions with limited ground-based measurements.

Key-Words: Land Surface Temperature, Air Temperature, Urban Heat Island, La Rioja, Argentina.

Received: May 31, 2024. Revised: December 15, 2025. Accepted: March 14, 2025. Published: April 23, 2025.

1 Introduction

The urban heat island effect (UHI) is a phenomenon where urban areas experience significantly higher temperatures than non-urban areas. This phenomenon is caused by factors such as the reduction of green cover, increased residual heat from human and productive activities, and the thermal characteristics of materials used in cities [0] Several authors argue that UHI is more pronounced in large cities due to the morphological characteristics of urban spaces, the building material´s optical and thermal properties, low vegetation levels, and the high contribution of anthropogenic heat [1].

This phenomenon has numerous negative impacts, such as reduced productivity, increased extreme weather events that can result in mortality, and higher electricity consumption with its subsequent economic impact [2]. Additionally, UHI contributes to global warming by intensifying the effects of climate change [3].

In natural desert environments, characterized by wide daily temperature fluctuations, low humidity, and, depending on the time of year, occasional strong winds, indoor spaces' comfort and habitability rely heavily on air conditioning systems. These systems are essential for counteracting high temperatures and ensuring suitable living conditions for inhabitants [4].

To estimate air temperature in forested areas and understand its relevance to urban heat island studies, it is pertinent to consider the work of [5], who used machine learning models to estimate air temperature from surface temperature on the forested slopes of Kilimanjaro. Their research demonstrates how machine learning models can enhance air temperature estimation in areas with limited weather station coverage, offering significant implications for understanding climate change and mitigating its effects in urban and rural environments [5].

1.1 Background of the Urban Heat Island

The study of the urban heat island (UHI) phenomenon originated in England. In 1833, Luke Howard observed temperature differences of 0.87°C between London and Greenwich, two locations separated by 13 km [6]. Thirty years later, research on this phenomenon began in France [7].

In 1958, Gordon Manley introduced the term "urban heat island" to describe the phenomenon, which remains in use today [7]. Until the early 1970s, research on Urban Heat Islands (UHIs) relied primarily on in situ temperature measurements.

With advancements in satellite technology, the UHI effect began to be studied using images captured by artificial satellites at an orbital altitude of 917 km. In 1972, [8] conducted the first studies using images captured by the Landsat 1 satellite (initially called ERTS-1—Earth Resources Technology Satellite).

1.2 Geographical Scope of the UHI

Regarding the geographical variability, UHI studies can be conducted at local scales, such as within a single city [6] [9] or an area [10], or at broader, more global scales [11] [12] [13]. Many local-scale studies use surrounding rural or peri-urban areas as a reference for spatial analysis.

Although the UHI pattern is associated with the location of cities, it is significantly influenced by direct solar radiation and anthropogenic activities. For this reason, vegetated areas play a critical role in restoring part of the energy and reducing the temperature gradient.

The UHI is not associated with a specific period. Urban heat islands can occur at night, often related to the absorption of solar energy throughout the day and the absence of thermal dissipation [13]. In contrast to the UHI effect, there is the urban cold island (UCI) effect, which analyzes the use of various materials, covers, and vegetation to mitigate UHI effects [14] [15].

1.3 Methods for Determining Urban Heat Islands (UHI)

Various methods are employed to assess the phenomenon of urban heat islands (UHIs). One approach involves the direct measurement of air temperature (Ta), which is instrumental in establishing the presence of UHIs.

Alternatively, satellite imagery can be utilized to measure Land Surface Temperature (LST) and evaluate the effects of surface urban heat islands (SUHI). Each method presents distinctive advantages and limitations, which will be discussed in the following sections.

Measurement of Air Temperature in Urban Heat Islands (UHI) is conducted in situ using temperature sensors, fixed weather stations, and mobile weather stations equipped in vehicles specifically designed for this purpose to measure temperature transects [9].

Measurement of Land Surface Temperature (LST) to evaluate the effect of surface urban heat islands (SUHI). This technique gained momentum starting in 2005 [16] and is generally carried out through data acquisition derived from the analysis of images taken by satellites.

1.4 Advantages and Disadvantages of Different Heat Island Measurement Methods

Although UHI and SUHI are used in urban climate studies, in situ air temperature measurements and satellite-derived surface temperatures are not directly comparable [17].

In situ UHI measurements offer high data accuracy and frequent measurement intervals, but their limited spatial coverage restricts the monitoring of large areas. These data support studies at various spatial scales, including historical analyzes [18], and allow for detailed geographical and temporal assessments of urban surface warming [17].

Thermal satellite remote sensing measures surface UHI and provides consistent, repeatable observations of the Earth's surface.

The use of satellite remote sensing to analyze Urban Heat Islands (SUHIs) faces several challenges, such as temporal discrepancies in data acquisition, limitations to daytime coverage, interference from clouds and vegetation, the need for atmospheric corrections to ensure accuracy, the effect of capture angles on radiances, and the difficulty of combining data of different resolutions and formats. In homogeneous rural environments, land surface temperature (LST) is generally a reliable predictor of air temperature. Nevertheless, this relationship depends on cloud cover, wind, time of day, season, and surrounding land cover [18].

Many studies use satellite-derived data to calculate urban heat islands. However, the spatial resolution of this data (0.5º x 0.5º, equivalent to an area of 2,651 km²) is broad, making it difficult to identify local variations. To overcome this limitation, it is necessary to compare satellite temperatures with measurements from ground-based weather stations. This approach allows for adjustments to the satellite data, improving its accuracy in assessing phenomena such as urban heat islands at the local scale.

The absence of previous studies and the limited network of in situ meteorological stations in La Rioja province necessitate a methodology grounded in satellite data analysis to assess the urban heat island (UHI) effect. This strategy will address data limitations and improve understanding of the phenomenon in the region.

Therefore, it is essential to determine the correction factor that enables the use of satellite data in measuring phenomena like the heat island effect (UHI) and estimating air temperatures in areas where there are no adequate means for direct measurements [19] [20].

The objective of this study is to develop a correction equation to transform land surface temperatures (LST) obtained from satellite data into more accurate air temperatures (Ta), using hourly data from two weather stations: one in the urban area of La Rioja (UA) and another in a non-urban area (NUA) of the same city. Additionally, the study aims to establish diurnal and nocturnal correlations between Ta and LST data for both geographic locations (UA and NUA) to optimize the interpretation of temperatures and improve the accuracy of Ta estimates from satellite data.

2 Methodology

This study uses diverse data sources to examine the disparities between air temperature (Ta) and land surface temperature (LST), revealing patterns associated with urban and rural environments.

2.1 Data Sources

- **Urban Air Temperature (TaUA):** Hourly temperature data for the urban area of La Rioja city were acquired from the National Meteorological Service station [23] located at the local airport (coordinates: -29.38 S, -66.79 W).
- **Rural Air Temperature (TaNUA):** Hourly temperature data for the non-urban area (NUA) were collected from a meteorological station situated 10 km from the La Rioja urban center (coordinates: -29.47 S, -66.78 W) (Fig. 1).
- **Land Surface Temperature (LST):** LST data were obtained from the NASA Global Modeling and Assimilation Office (GMAO MERRA-2) Atmospheric Reanalysis Model, representing hourly dry bulb temperature at 2 meters [20] [21]. Due to the 0.5º x 0.5º spatial resolution of the satellite data [21], approximately 55.5 km in latitude and 48.2 km in longitude at this location, a single LST value was applied to both urban and rural areas, as the meteorological stations are within this resolution.
- **Measurement Height:** All meteorological station measurements were recorded at 2 meters, adhering to the recommendation by [19].

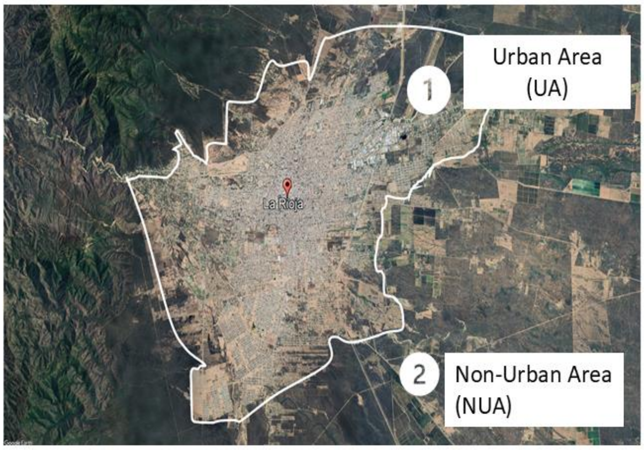

Fig. 1: Map of La Rioja, Argentina, highlighting the analyzed areas. The Urban Area (UA) (1) and Non-Urban Area (NUA) (2) of La Rioja city are demarcated. Source: Google Earth.

2.2 Data Processing

The data processing included the following steps:

- A total of 26,277 temperature data points were classified and organized into daytime and nighttime measurements.
- The classification criteria for daytime hours were based on the time frame between 8:00 AM and 6:00 PM. Nighttime data corresponded to the hours from 7:00 PM to 7:00 AM.

2.3 Analysis of Classified Data

Descriptive statistical analysis was performed, calculating mean values, standard deviations, and the temperature range, identifying the year's median, maximum, and minimum values. Additionally, the temperature differences between the urban area (UA) and Land Surface Temperature (LST) were calculated, analyzing patterns consistent with the temperature differences between the two data sources, following the methodology described in previous studies [22][24].

The same procedure was applied to determine the temperature differences between NUA and LST. To validate the data, a K-fold cross-validation (k=20) approach was implemented, calculating the Root Mean Square Error (RMSE) to evaluate the accuracy of the regression models.

Furthermore, a sensitivity analysis was conducted by applying perturbations of ±0.5 °C to air temperature measurements. A new linear regression model was computed for each perturbation, determining the updated regression parameters (slope and intercept) and recalculating the coefficient of determination (R^2). This allowed for assessing how variations in air temperatures impact the correlation between LST and Ta.

This study employed linear regression analysis to examine the relationship between the satellite-derived Land Surface Temperature (LST) and the air temperatures (Ta) measured at weather stations in UA and NUA. This analysis enables the development of a correction model to adjust for discrepancies between LST and Ta (for both UA and NUA), thereby improving the accuracy of temperature estimations derived from satellite data.

Linear regression will also help establish the daytime and nighttime correlation between the variables, providing insights into how temperatures fluctuate throughout the day and optimizing the interpretation of satellite data in the two different locations (UA and NUA). Additionally, the coefficient of determination (R^2) was calculated to assess the strength and quality of the relationship between Land Surface Temperature (LST) and air temperatures (Ta).

3 Results

3.1 Analysis of Continuous 24-Hour Temperature Data for the Urban Area (UA) in 2021.

A descriptive statistical analysis was conducted for the urban area (UA) of La Rioja city. The analyzed sample comprised daily measurements of urban air temperature (Ta_{UA}) and their corresponding differences from satellite-derived land surface temperature (LST_{UA}) (Table 1). The distribution of these temperature differences ($\Delta T_{UA} = Ta_{UA} - LST_{UA}$) is further illustrated in Fig. 2.

Fig. 2 depicts the distribution of temperature differences (ΔT_{UA}), where positive values indicate instances in which Ta_{UA} exceeded LST_{UA}. This disparity highlights potential limitations of satellite-based LST_{UA} measurements in capturing localized air temperature variations. The observed concentration of data points with positive ΔT_{UA} suggests a systematic underestimation of air temperature by the LST_{UA} values.

Table 1: Annual Descriptive Statistical Data for Air Temperature in the Urban Area (Ta_{UA}) and Its Differences from Satellite-Measured Land Surface Temperature (LST_{UA}).

	Ta_{UA}	LST_{UA}	ΔT_{UA} = (Ta_{UA} – LST_{UA})
Daily Average (ºC)	20.43	19.63	0.80
Standard Deviation (ºC)	7.95	7.72	2.51
Maximum Recorded Temperature (ºC)	40.80	38.95	-
Minimum Recorded Temperature (ºC)	-3.90	-0.42	-
Median (ºC)	20.90	19.68	-
Mode	21.40	21.90	-

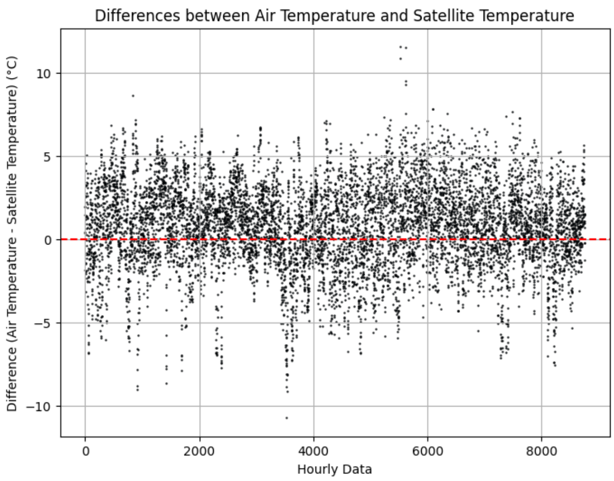

Fig. 2: Temperature differences between Ta_{UA} and LST_{UA}. Note: Positive values indicate Ta_{UA} > LST_{UA}.

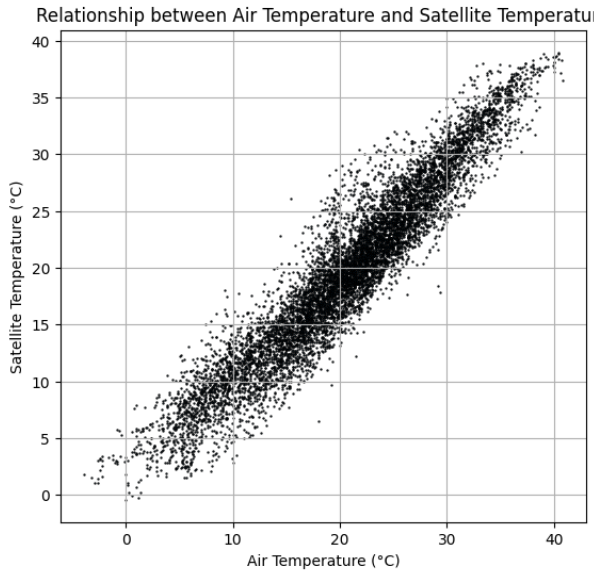

Fig. 3: Regression Analysis of Ta_{AU} – LST.

From the statistical processing of 8,760 hourly data pairs, consisting of Ta_{UA} and LST_{UA}, a regression analysis yielded an $R^2 = 0.9011$. The following equation was obtained, relating LST_{UA} to Ta_{UA} (Fig. 3):

$$LST_{UA} = 0.9229\ Ta_{UA} + 0.7747 \quad (1)$$

Equation 1 allows for the prediction of LST_{UA} temperatures based on Ta_{UA} for the urban area of La Rioja. Similarly, Ta_{UA} can also be calculated from LST data using Equation 2:

$$Ta_{UA} = (LST_{UA} - 0.7747) / 0.9229 \quad (2)$$

K-fold cross-validation results revealed a mean correlation of 0.9492, with a standard deviation of 0.0002 and a standard error of the mean of 0.0001, demonstrating the model's reliability. A sensitivity analysis was also performed, assessing the model's stability under temperature perturbations of -0.50 °C, 0.00 °C, and +0.50 °C. The R^2 value remained consistent at 0.9011 across these perturbations, suggesting that the regression model is robust and stable against minor temperature variations. The root mean square error (RMSE) is 2.6327.

3.2. Analysis of Continuous 24-Hour Temperature Data for the Non-Urban Area (NUA) in 2021.

For NUA of the city of La Rioja, a descriptive statistical analysis was conducted (Table 2).

The analyzed sample corresponds to the total air temperature measurements (Ta_{NUA}) and satellite measurements (LST_{NUA}). Additionally, the differences between the measurements of Ta_{NUA} and LST_{NUA} were determined (Fig. 4).

Table 2. Annual Descriptive Statistical Data for Air Temperature in the Non-Urban Area (Ta_{NUA}) and Its Differences from Satellite-Measured Land Surface Temperature (LST_{NUA}).

	Ta_{NUA}	LST_{NUA}	ΔT_{NUA} = (Ta_{NUA} – LST_{NUA})
Annual Daily Average (°C)	19.46	19.63	-0.17
Standard Deviation (°C)	8.64	7.72	3.13
Maximum Recorded Temperature (°C)	41.00	38.95	-
Minimum Recorded Temperature (°C)	-6.10	-0.42	-
Median (°C)	19.90	19.68	-
Mode	19.80	21.90	-

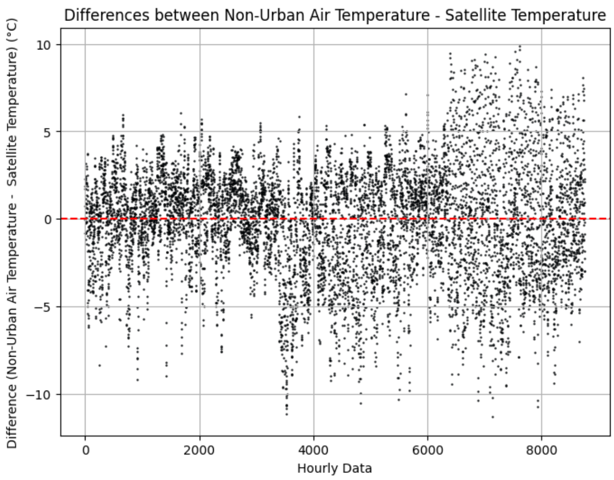

Fig. 4: Temperature differences between Ta_{NUA} and LST. Note: Positive values indicate $Ta_{NUA} > LST_{NUA}$.

The temperature differences between Ta_{NUA} and LST_{NUA} were plotted, as shown in Fig. 4. Positive values indicate that Ta_{NUA} exceeds LST_{NUA}, highlighting instances where the ambient air temperature in the non-urban area is higher than the satellite-derived land surface temperature. This discrepancy may reflect the limitations of satellite-based measurements in capturing localized variations in air temperature.

A significant density of measurements where Ta_{NUA} is higher than LST_{NUA} can be observed, suggesting that the calculated LST_{NUA} values are underestimated. This phenomenon is evident throughout all months, with the largest temperature differences occurring during the winter and summer.

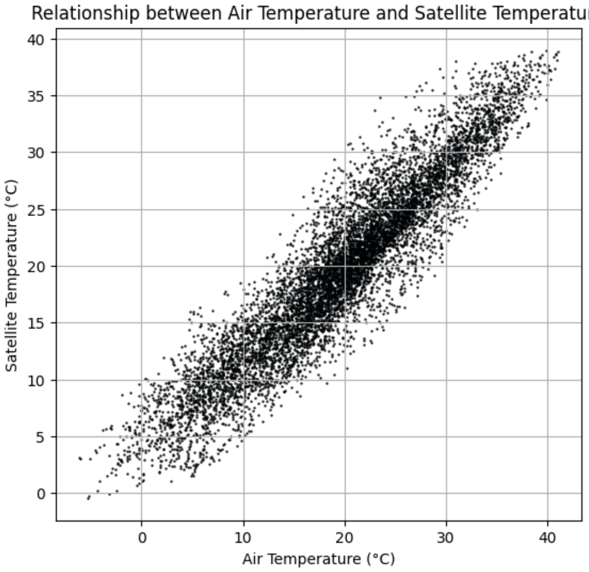

Fig. 5: Regression analysis for data A) Ta_{NUA} – LST_{NUA}.

Based on the analysis of the NUA data (Fig. 5), a regression was obtained with $R^2 = 0.8701$ (Equations 3 and 4):

$$LST_{NUA} = 0.8337\ Ta_{NUA} + 3.496 \quad (3)$$

$$Ta_{NUA} = (LST_{NUA} - 3.4096) / 0.8337 \quad (4)$$

K-fold cross-validation results revealed a mean correlation of 0.9328, with a standard deviation of 0.0003 and a standard error of the mean of 0.0001, demonstrating the model's reliability. A sensitivity analysis was also performed, assessing the model's stability under temperature perturbations of -0.50 °C, 0.00 °C, and +0.50 °C. The R^2 value remained consistent at 0.8701 across these perturbations, suggesting that the regression model is robust and stable against minor temperature variations. The root mean square error (RMSE) is 3.3398.

3.3- Analysis of daytime temperature data for the urban area (UA) and non-urban area (NUA) for 2021.

For the diurnal temperature variation, statistical analyzes were conducted on the data for Ta_{UA}, Ta_{NUA}, LST_{UA}, and LST_{NUA} between 8 AM and 6 PM (Table 3).

Table 3. Annual Diurnal Descriptive Statistical Data for the Non-Urban Area (NUA) and Urban Area (UA).

	Ta_{UA}	Ta_{NUA}	LST	(ΔT_{UA}= Ta_{UA} – LST)	(ΔT_{NAU}= Ta_{NUA} – LST)
Annual daily mean (ºC)	23,04	23,29	22,37	0,66	0,92
Standard deviation (ºC)	7,74	8,16	7,88	2,54	2,88
Maximum temperature recorded (ºC)	40,80	41,00	38,95	11,48	9,87
Minimum temperature recorded (ºC)	-3,20	-6,10	0,89	-10,70	-10,20
Median (ºC)	23,00	23,50	22,90	0,82	1,17

The mean air temperatures show that in the urban area (Ta_{UA}) and the non-urban area (Ta_{NUA}) of La Rioja, air temperatures are similar, with values of 23.04 °C and 23.29 °C, respectively. However, the land surface temperature (LST) is slightly lower, with an average of 22.37 °C (Fig. 6).

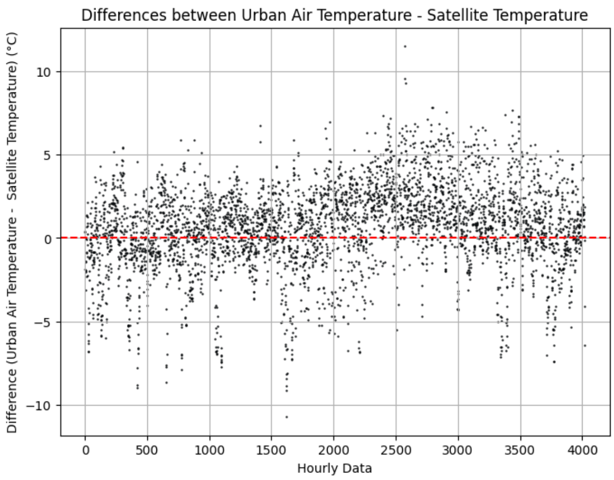

Fig. 6: Diurnal temperature differences between Ta_{UA} and LST_{UA}. Note: Positive values indicate $Ta_{UA} > LST_{UA}$.

The diurnal differences between air temperatures and LST indicate that, on average, air temperatures are higher than the satellite-measured land surface temperatures, with a larger difference in the non-urban area (ΔT_{NUA} = 0.92 °C) compared to the urban area (ΔT_{UA} = 0.66 °C).

Regarding variability, the diurnal differences present a significant standard deviation (2.54 °C for ΔT_{UA} and 2.88 °C for ΔT_{NUA}), indicating notable fluctuations in temperature differences between Ta_{UA}, Ta_{NUA}, and LST over time. The data suggest that land surface temperature (LST) tends to underestimate air temperatures, especially on warmer days when the most significant discrepancies are observed.

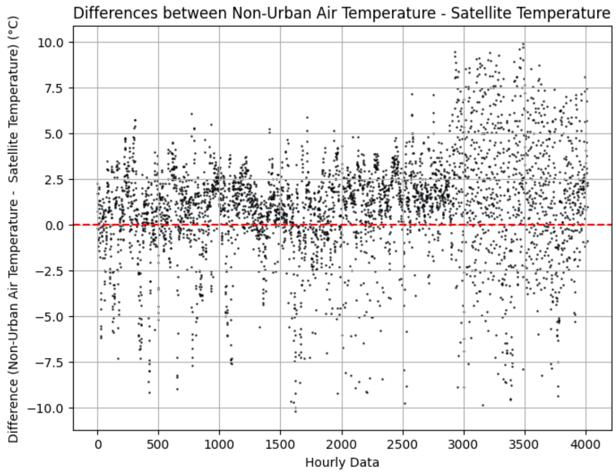

Fig. 7: Diurnal temperature differences between Ta_{NUA} and LST. Note: Positive values indicate Ta_{NUA} > LST.

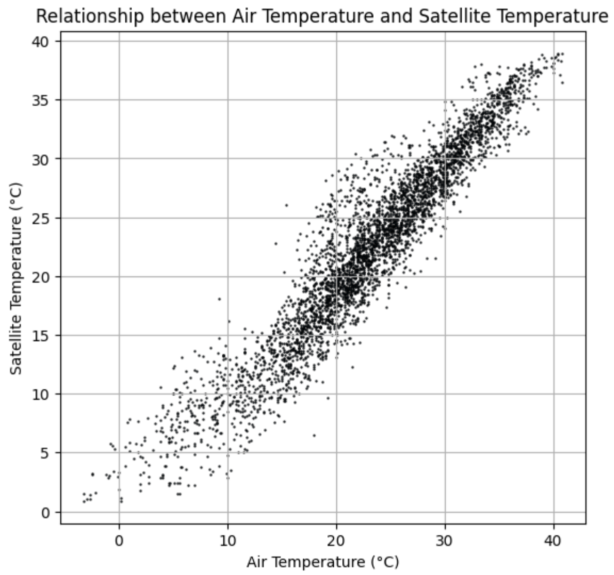

Fig. 8: Regression analysis for diurnal data A) Ta_{UA} – LST_{UA}.

Based on the analysis of Ta_{UA} and Ta_{NUA} data versus LST (Fig.s 8 and 9), a regression was obtained with R^2 = 0.8975 (Equation 5—Fig. 8) and R^2 = 0.8766 (Equation 6—Fig. 9).

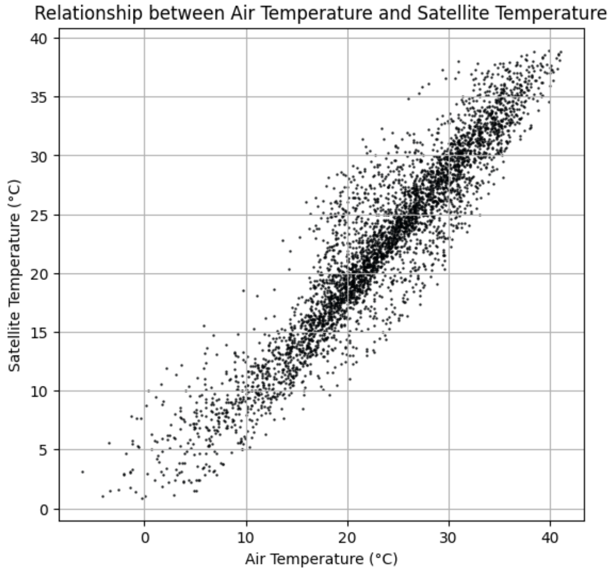

Fig. 9: Regression analysis for diurnal data Ta_{NUA} – LST_{NUA}

$$LST_{UA} = 0.9640\ Ta_{UA} + 0.1569 \quad (5)$$

In the daily UA analysis, the K-fold cross-validation approach produced a mean correlation of 0.9464, with low variability reflected in a standard deviation of 0.0004 and a standard error of 0.0001. A sensitivity analysis examined model performance under temperature deviations of -0.50 °C, 0.00 °C, and +0.50 °C to further assess model robustness. The results demonstrated that the R^2 value remained unchanged at 0.8975, underscoring the model's stability against small thermal perturbations. The root mean square error (RMSE) is 2.6179.

$$LST_{NUA} = 0.9045\ Ta_{NUA} + 1.3067 \quad (6)$$

On the other hand, for the daily NUA analysis, the K-fold cross-validation procedure demonstrated a mean correlation of 0.9363, with minimal variability, as indicated by a standard deviation of 0.0005 and a standard error of 0.0001. Furthermore, a sensitivity analysis was performed to evaluate the model's performance under temperature fluctuations of -0.50 °C, 0.00 °C, and +0.50 °C. The results showed that the R^2 value remained constant at 0.8766, reinforcing the model's stability against small thermal perturbations. The root mean square error (RMSE) is 3.0596.

3.4 Nocturnal Temperature Data Analysis for Urban (UA) and Non-Urban Areas (NUA) in 2021. To analyze nocturnal temperature variations, the Ta_{UA}, Ta_{NUA}, and LST data were statistically evaluated between 7:00 PM and 7:00 AM (Table 4).

Table 4. Annual descriptive statistics for nocturnal temperatures in the non-urban area (NUA) and their differences with LST.

	Ta_{UA}	Ta_{NUA}	LST	(ΔT_{UA}= Ta_{UA} – LST)	(ΔT_{NAU}= Ta_{NUA} – LST)
Annual nocturnal mean (ºC)	18.23	16.21	17.31	0.92	-1.10
Standard deviation (ºC)	7.44	7.66	6.78	2.47	3.04
Maximum temperature recorded (ºC)	39.10	37.60	37.65	11.55	8.39
Minimum temperature recorded (ºC)	-3.90	-6.00	-0.42	-8.06	-11.32
Median (ºC)	18.80	17	17.57	0.99	-1.07

The data indicate that annual average nighttime temperatures in the urban area (Ta_{UA}) are higher than in the non-urban area (Ta_{NUA}), with values of 18.23 ºC and 16.21 ºC, respectively. The LST (17.31 ºC) lies between these values, being underestimated relative to Ta_{UA} and overestimated in the case of Ta_{NUA}. The maximum and minimum recorded temperatures also reflect these trends, with higher maxima in the urban area and greater nighttime cooling in the non-urban area.

Nighttime temperature differences between Ta_{UA} and LST show significant fluctuations, with positive values indicating that Ta_{UA} is more considerable than LST and negative values indicating the opposite. The temperature differences range from -7.5℃ to 12.5℃ throughout the nocturnal hourly data collected between January 2021 and December 2021. This analysis reveals considerable variability in the nocturnal differences between the two measurement sites, especially in the non-urban area, indicating fluctuations in the nighttime temperature differences between Ta_{NUA} and LST (Fig. 10 and 11).

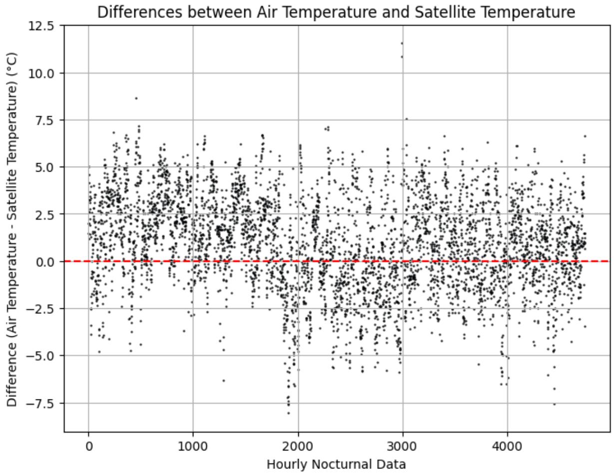

Fig. 10: Nighttime temperature differences between Ta_{UA} and LST.

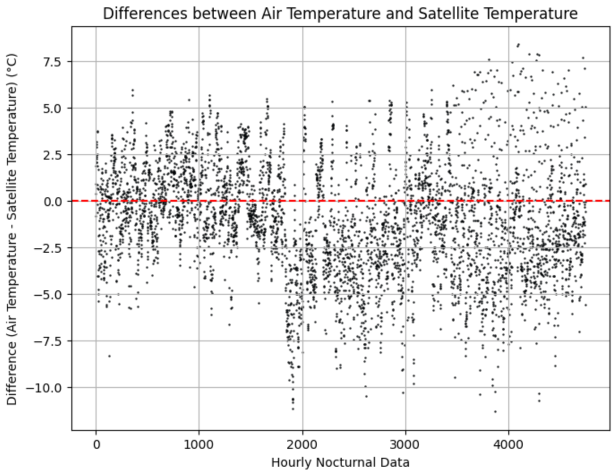

Fig. 11: Nighttime temperature differences between Ta_{NUA} and LST. Note: Positive values indicate Ta_{NUA} > LST.

Overall, air temperatures in the urban area are higher and more stable than those in the non-urban area, exhibiting greater variations and more pronounced cooling. These findings suggest significant thermal differences between urban and non-urban areas, as well as between air temperatures and land surface temperatures.

In this study, we analyzed the correlation between land surface temperature (LST) and air temperature (Ta) using a regression equation defined (Equations 7 and 8—Fig. 12).

$$LST_{UA} = 0.8595\ Ta_{UA} + 1.6422 \quad (7)$$

The results indicate a strong positive correlation R^2= 0.8906. The root mean square error (RMSE) is 2.6081. The equation for calculating Ta_{UA} from LST is given by

$$Ta_{UA}= 0.8595/ (LST −1.6403) \quad (8)$$

K-fold cross-validation results revealed a mean correlation of 0.9437, with a standard deviation of 0.0003 and a standard error of the mean of 0.0001, demonstrating the model's reliability.

A sensitivity analysis was also performed, assessing the model's stability under temperature perturbations of -0.50 °C, 0.00 °C, and +0.50 °C. The R^2 value remained consistent at 0.8906 across these perturbations, suggesting that the regression model is robust and stable against minor temperature variations.

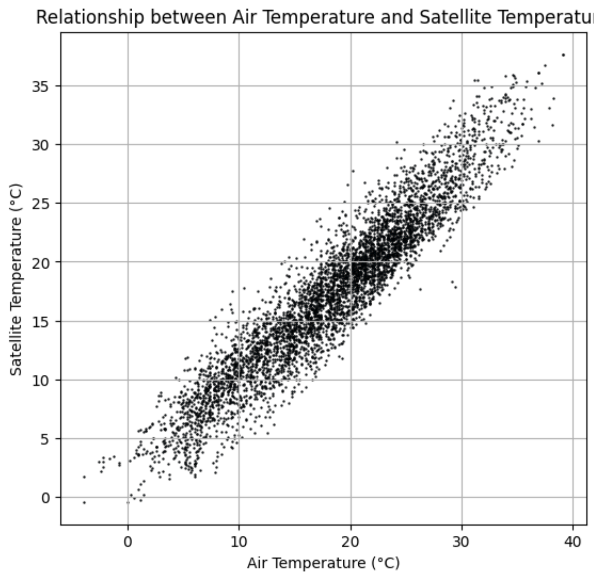

Fig. 12: Regression analysis for nighttime data: Ta_{UA} – LST.

The analysis of the dataset using Pearson's correlation revealed the equation.

$$LST=0.8122\ Ta_{NUA} +4.1415 \quad (9)$$

The R^2 value of 0.8433 indicates a strong relationship between land surface temperature (LST) and air temperature in non-urban areas (Ta_{NUA}). The corresponding equation for Ta_{NUA} based on LST is

$$Ta_{NUA} = 0.8122/(LST−4.1415) \quad (10)$$

with a root mean square error (RMSE) of 3.3035, reflecting a moderate level of predictive accuracy.

K-fold cross-validation was employed to validate the model, resulting in an average correlation of 0.9183, a standard deviation of 0.0005, and a standard error of the mean of 0.0001, which supports the model's reliability.

Sensitivity analysis indicated that perturbations of -0.50°C, 0.00°C, and +0.50°C resulted in consistent equations with an R^2 value remaining at 0.8433 (Equations 9 and 10—Fig. 13). These results highlight the regression model's robustness against minor temperature variations.

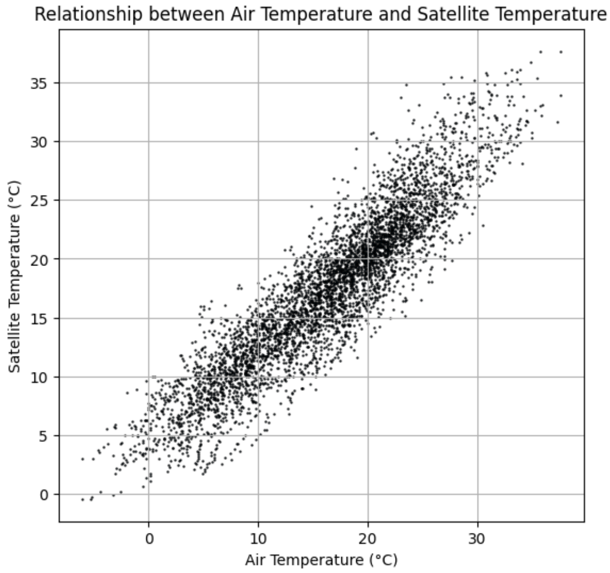

Fig. 13: Regression analysis for nighttime data: Ta_{NUA} – LST.

4 Conclusion

The objective of this study was to develop a correction equation to transform land surface temperatures (LST) obtained from satellite data into air temperatures (Ta) in the urban area of the city of La Rioja (UA) and another for a non-urban area (NUA).

To achieve this, equations were derived to calculate air temperature (Ta) values based on land surface temperatures (LST) from satellite data sources.

The results show that, in general, LST underestimates air temperatures (Ta) in both areas, with more pronounced differences during the summer months. The equations derived from the regression analysis, with determination coefficients (R^2) over 0.87, enable reliable predictions of air temperatures based on satellite data, thereby improving the accuracy of Ta estimates.

The underestimation of air temperatures (Ta) by land surface temperatures (LST) can be attributed to several factors. Firstly, LST is derived from satellite observations, which represent the temperature of the Earth's surface [18] [19] [20]. At the same time, Ta is measured at a height above the surface [9], influenced by local microclimates [25], leading to discrepancies. Additionally, in areas with significant vegetation, the cooling effect of evapotranspiration can decrease surface temperatures, resulting in LST readings that do not reflect the warmer air temperatures. To add complexity to the Ta-LST relationships, an increasing spatial variation in LST was found during the day for land covers of tall and short trees [25]. Different land cover types, such as urban areas, can also affect heat absorption and release, with urban heat island effects causing higher air temperatures not captured by LST [25]. Furthermore, atmospheric conditions such as humidity, wind, and cloud cover can impact the relationship between LST and Ta, with high moisture potentially leading to warmer air temperatures that LST does not account for. Lastly, limitations of the sensors used to measure LST can introduce biases, ultimately affecting the accuracy of temperature predictions based on satellite data.

Additionally, daytime and nighttime data were correlated between Ta and LST for both geographical locations (UA and NUA) to optimize the interpretation of temperatures and enhance the precision of Ta estimates derived from satellite data.

The analysis of diurnal and nocturnal temperature patterns revealed thermal variation, highlighting that air temperatures in the urban area (UA) are higher and more stable than in the non-urban area (NUA), which exhibits greater fluctuations and more pronounced nighttime cooling.

These findings highlight the importance of adjusting LST data according to geographic and temporal contexts to obtain more accurate estimates of air temperatures, which may have significant implications for climate studies and environmental management in urban and rural areas.

This study is particularly valuable for various sectors, including agriculture, public health, and urban planning. By providing a reliable method to estimate air temperatures (Ta_{AU} and Ta_{NUA}) from satellite data, it supports farmers in monitoring temperature variations that impact crop growth, aids public health officials in assessing heat-related risks, and assists urban planners in designing more resilient and sustainable cities, especially in regions like La Rioja, where ground-based temperature measurements are limited.

Acknowledgement:
The authors would like to express their gratitude to Mercedes Frassinelli for the translation and revision of this manuscript.

References:

[1] United Nations. (2021). *Environment Programme Beating the heat: A sustainable cooling handbook for cities*. Nairobi.

[2] Colli, M. F., Correa, É. N., & Martínez, C. F. (2020). Aplicación del método WUDAPT en la ciudad de Mendoza, Argentina, para definir zonas climáticas locales. *Urbano*, 23(42), 18-31. https://dx.doi.org/10.22320/07183607.2020.23.42.02

[3] United Nations (2021). *United Nations climate change annual report 2021*. UNFCCC. https://unfccc.int/sites/default/files/resource/UNFCCC_Annual_Report_2021.pdf

[4] Lovriha, I. M. (2022). Una revisión sobre la isla de calor urbana y sus particularidades en zonas desérticas de México. *Vivienda y comunidades sustentables*, (12), 9-25.

[5] Saif, J., Wright, A., Khattak, S., & Elfadli, K. (2021). Keeping Cool in the Desert: Using Wind Catchers for Improved Thermal Comfort and Indoor Air Quality at Half the Energy. *Buildings,* 11(3), 100. https://doi.org/10.3390/buildings11030100

[6] Forooshani, M., Gegov, A., Pepin, N., & Adda, M. (2022). Modeling air temperature in forested areas using machine learning. *WSEAS Transactions on Computers*, 21, 23-30. https://doi.org/10.37394/23205.2022.21.23

[7] Aragón, J. A. ., Rodríguez, E. D. ., Varon , G. . A., & Sánchez, G. A. (2020). Análisis de islas de calor por medio de imágenes satelitales y SIG en el área urbana de la Sabana de Bogotá. *Geographicalia,* (72), 39–64. https://doi.org/10.26754/ojs_geoph/geoph.2020724571

[8] Moreno García, M. del C. (1990). Bibliografía sobre climatología urbana: La "isla de calor", I. *Revista de Geografia,* 24(1-2). Recuperado de http://www.raco.cat/index.php/RevistaGeografia/article/view/46055

[9] Rao, P. K., Smith, W. L., & Koffler, R. (1972). Global sea-surface temperature distribution determined from an environmental satellite. Monthly *Weather Review,* 100(1), 10–14. https://doi.org/10.1175/1520-0493(1972)100

[10] Asar, M. L., Estallo, E. L., Benitez, E. M., Di Benedetto, H. M., & Ludueña Almeida, F. (2021). La UHI urbano entre 2018 y 2020 en la ciudad de Córdoba, Argentina. En G. A. Monti (Colab.), *106° Reunión de la Asociación Física Argentina: Segundo Webinar* (p. 286). Asociación Física Argentina.

[11] Ruiz, M. A., Colli, M. F., Martinez, C. F., & Correa-Cantaloube, E. N. (2022). Park cool island and built environment: A ten-year evaluation in Parque Central, Mendoza-Argentina. *Sustainable Cities and Society*, 79,

103681. https://doi.org/10.1016/j.scs.2022.103681.

[12] Parastatidis, D., Mitraka, Z., Chrysoulakis, N., & Abrams, M. (2017). Online global land surface temperature estimation from Landsat. *Remote Sensing,* 9(12), 1208. https://doi.org/10.3390/rs9121208

[13] Chakraborty, T., & Lee, X. (2019). A simplified urban-extent algorithm to characterize surface urban heat islands globally and examine vegetation control on their spatiotemporal variability. International *Journal of Applied Earth Observation and Geoinformation,* 74, 269–280. https://doi.org/10.1016/j.jag.2018.09.015

[14] Casadei, P., Semmartin, M., & Garbulsky, M. F. (2021). Análisis regional de las islas de calor urbano en la Argentina. *Ecología Austral,* 31(1), 190–203. https://doi.org/10.25260/EA.21.31.1.0.970

[15] Xu, C., Wang, W., & Zhu, H. (2024). Spatial gradient differences in the cooling island effect and influencing factors of urban park green spaces in Beijing. *Buildings,* 14(5), 1206. https://doi.org/10.3390/buildings14051206

[16] Zhou, B., Erell, E., Hough, I., Rosenblatt, J., Just, A. C., Novack, V., & Kloog, I. (2020). Estimating near-surface air temperature across Israel using a machine learning based hybrid approach. *International Journal of Climatology*: *A Journal of the Royal Meteorological Society*, 40(14), 6570. https://doi.org/10.1002/joc.6570

[17] Berg, E.; Kucharik, C. (2022) The Dynamic Relationship between Air and Land Surface Temperature within the Madison, Wisconsin Urban Heat Island. *Remote Sens*.2022 14, 165. https://doi.org/10.3390/rs14010165

[18] Lozada Montanari, M. S., & Camilloni, I. (2022). Variabilidad espacio-temporal de la isla de calor superficial en tres ciudades argentinas. *Meteorológica,* 47(1), e012. https://doi.org/10.24215/1850468Xe012

[19] Weng, Q., & International Society for Photogrammetry and Remote Sensing. (2009). Thermal infrared remote sensing for urban climate and environmental studies: Methods, applications, and trends. *ISPRS Journal of Photogrammetry and Remote Sensing*, 64, 335–344. https://doi.org/10.1016/j.isprsjprs.2009.03.007

[20] Rosenfeld, A., Dorman, M., Schwartz, J., Novack, V., Just, A. C., & Kloog, I. (2017). Estimating daily minimum, maximum, and mean near surface air temperature using hybrid satellite models across Israel. *Environmental Research,* 159, 297-312. https://doi.org/10.1016/j.envres.2017.08.017

[21] Zoran, M. A., Savastru, R., Savastru, D., Tautan, M. N., & Penache, A. C. (2023). Synergy of time series-derived satellite biophysical parameters and in-situ monitoring data for urban heat management: A case study of Bucharest. *WSEAS Transactions on Environment and Development*, 19, 1038-1051. https://doi.org/10.37394/232015.2023.19.98

[22] NASA. (2024). Daily availability data. *NASA POWER Project*. https://power.larc.nasa.gov/dashboard/availability/daily/

[23] Orellana Samaniego, M. (2020). *Estimación de la temperatura mensual del aire usando imágenes satelitales en una zona de topografía muy variable en los Andes del sur del Ecuador* (Thesis, Universidad Nacional de Colombia). Universidad Nacional de Colombia.

[24] SMN (2024) *Datasets del servicio meteorológico nacional*.

[25] Crum, S. M., & Jenerette, G. D. (2017). Microclimate variation among urban land covers: The importance of vertical and horizontal structure in air and land surface temperature relationships. *Journal of Applied Meteorology and Climatology*, *56*(9), 2531–2543. https://doi.org/10.1175/JAMC-D-17-0054.1

[26] Hinojosa Guzmán, B., Maillard, O., & Saucedo, D. (2021). Land surface temperature and climatic scenarios for land use change in the metropolitan municipalities of the department of Santa Cruz, Bolivia. *Ecología en Bolivia,* 56(1), 17-28. https://doi.org/ISSN 20075-5023

Contribution of Individual Authors to the Creation of a Scientific Article (Ghostwriting Policy)

The authors equally contributed to the present research, at all stages from the formulation of the problem to the final findings and solution.

Sources of Funding for Research Presented in a Scientific Article or Scientific Article Itself

The authors express their gratitude to the Universidad Nacional de La Rioja for funding the project "Study of the Urban Heat Island Effect in the City of La Rioja," Project 27/A841.

Conflict of Interest

The authors have no conflicts of interest to declare that are relevant to the content of this article.